sustainability

MDPI

Article

Study on Anchoring Characteristics and Freeze–Thaw Degradation Law of the Cement-Based Early-Strength Anchor in Freeze–Thaw Regions

Ming Yang [1,2,*], Shenggui Deng [3] and Zizhang Dong [4]

[1] Institute of Geotechnical Engineering, School of Transportation, Southeast University, Nanjing 210096, China
[2] Nanjing Public Project Construction Center, Nanjing 210019, China
[3] College of Marine Geosciences, Ocean University of China, Qingdao 266100, China
[4] College of Environmental Science and Engineering, Ocean University of China, Qingdao 266100, China
* Correspondence: yangming20220101@163.com

Abstract: This article focuses on the effect of freeze–thaw cycling on a cement-based early-strength anchor material, the compressive strength of which at 24 h is 14 times that of ordinary cement, and the compressive strength at 7 h is twice that of ordinary cement. The setting time required to achieve the expected strength is 1/7 of that of ordinary cement. Through indoor freeze–thaw cycling tests, the appearance changes, quality loss, strength loss, and microstructure changes in the early-strength anchor after 0, 5, 15, 25, 50, 75, and 100 cycles were studied, revealing the evolution of the mechanical properties and micromechanisms of the cement-based early-strength anchor material under freeze–thaw cycling conditions. The sample freeze–thaw failure criteria were determined, evaluation indicators reflecting the degree of damage were defined, and their relationships with the number of freeze–thaw cycles were fitted to assess the durability of the cement-based early-strength anchor material under freeze–thaw environments. This provides a theoretical reference for further improvements in material properties and adaption to different environments.

Keywords: anchor material; cement-based early-strength anchor material; strength degradation; freeze–thaw

Citation: Yang, M.; Deng, S.; Dong, Z. Study on Anchoring Characteristics and Freeze–Thaw Degradation Law of the Cement-Based Early-Strength Anchor in Freeze–Thaw Regions. *Sustainability* **2023**, *15*, 7773. https://doi.org/10.3390/su15107773

Academic Editors: Zhen Guo, Shengjie Rui and Wenjie Zhou

Received: 27 March 2023
Revised: 25 April 2023
Accepted: 5 May 2023
Published: 9 May 2023

1. Introduction

China has the third largest frozen soil area in the world, with the permafrost region accounting for 22.83% of the country's land area. A large number of engineering constructions are distributed in the permafrost region, and after grouting and other engineering operations, the cementitious materials face the adverse effects of freeze–thaw environments [1]. The grouting body of cementitious materials is a composite body consisting of solid, liquid, and gas phases. Under low-temperature conditions, water freezes and expands in volume, exerting pressure on the two walls of the grouting body's cracks. When the temperature rises, the ice melts into water, which penetrates into the interior of the structure through the pores on the surface of the grouting body, and at the same time, the pressure on the two walls drops sharply, causing a rebound [2]. The transformation between ice and water appears alternately on the surface and inside of the cementitious grouting body, and in repeated freeze–thaw cycles, the cracks will expand and increase, thereby affecting the mechanical properties of the cementitious materials [3].

The frost resistance of cement-based grouting materials is an important aspect of performance evaluation, and in recent years, many scholars have focused on research at low or ultra-low temperatures [4–6], as shown in Table 1.

Table 1. Previous scholars' research.

Researchers	Range of Freeze–Thaw Cycle Temperature/°C	Samples	Conclusion
Li [4]	Not mentioned	PVA-ECC and cement	After 110 cycles, the concrete specimens had severely deteriorated. ECC specimens survived the test duration of 300 cycles.
Najjar [5]	−18~85	CEAM	Applying freeze–thaw cycles reduced the fracture energy of CEAM.
Chen [6]	−20~5	porous cement	The evolution of FHS in the freezing process can be generally divided into three stages.
Zhang [7]	−60~20	hardened cement	The thermal deformation is mainly affected by the freezing or melting of pore solution in pores smaller than 8 nm.
Alsaif [8]	−15~20	SFRRuC	SFRRuC are able to withstand 56 freeze–thaw cycles with acceptable scaling and without presenting internal damage or degradation in mechanical performance.
Johannesson [9]	−80~20	cement	Damage occurs in the temperature range of about −10~−55 °C, when the air content is lower than about 4% of the total volume.

Among the scholars, Zhang et al. [7] innovatively explained the thermal deformation trend of concrete at low temperature by analyzing the freezing point of a bulk solution and pore solution in saturated hardened cement paste and found that the freezing of pore water in pores smaller than 8 nm is a key factor affecting the low-temperature thermal deformation of cement-based materials. With the increase in the water–cement ratio, the thermal strain and damage of cement-based grouting materials become more pronounced. Alsaif [8] evaluated the freeze–thaw performance of steel-fiber-reinforced rubberized concretes (SFRRuC) engineered for flexible concrete pavements. The results showed that SFRRuC are able to withstand 56 freeze–thaw cycles with acceptable scaling and without presenting internal damage or degradation in mechanical performance. Johannesson [9] investigated samples of concrete at different water-to-cement ratios and air contents subjected to freeze–thaw cycles with the lowest temperature of about −80 °C. By adopting a novel technique, a scanning calorimeter was used to obtain data from which the ice contents at different freeze temperatures could be calculated. The results showed that damage occurred in the temperature range of about −10 °C to −55 °C, when the air content was lower than about 4% of the total volume. In addition, an American scholar Powers [10,11] was the first to propose two theories of failure, namely, hydrostatic pressure failure theory and osmotic pressure failure theory.

Currently, there is a lack of research on the frost resistance of cement-based early-strength anchor material, which makes it difficult to accurately evaluate its performance changes when applied in the seasonal frozen zone environment. Freeze–thaw cycle testing is a powerful tool for studying the frost resistance and durability of materials. The objective of this study was to study the appearance changes, mass loss, strength loss, and microstructure changes in a cement-based early-strength anchor material through indoor freeze–thaw cycle experiments and to reveal the evolution of mechanical properties and microscopic mechanisms of the cement-based early-strength anchor material under freeze–thaw cycle conditions with a view to provide a theoretical reference for further improvements in material properties and adaption to different environments.

2. Materials and Methods

2.1. The Cement-Based Early-Strength Anchor Material

Cement-based early-strength anchor material is a newly developed composite cementitious material which has undergone independent research and development. The material ratio mainly includes main materials and auxiliary materials, from which, the main materials are, by mass, 40% sulfoaluminate cement, 20% early-strength Portland cement, 30% fine sand, 10% calcium sulfate, calcium carbonate, etc. Auxiliary materials include MgO, silica fume, naphthalene-based water reducer, boric acid, etc. The mixing standard used is a 0.28 water-to-material ratio.

The particle size distribution of cement-based cementitious materials is closely related to their mechanical properties [12–14]. A Winner3003 dry laser particle size analyzer was used to analyze the particle size distribution of the test material, and partial particle size parameters of the cement-based early-strength anchor material used in this study were obtained, as shown in Table 2. The particle diameters of 10%, 30%, and 60% of particles in this material were 4.661 μm, 14.509 μm, and 38.855 μm. The particle size of the material was relatively uniform, meaning the gradation of the material was poor. According to engineering experience, the grading of anchor cable grouting materials is generally poor, meaning the material met the grading requirements for anchor cable grouting materials.

Table 2. Particle size parameters.

Parameters	*d*10	*d*30	*d*50	*d*60	*d*90
value/μm	4.661	14.509	29.987	38.855	195.195

2.2. Preparation of Compressive Strength Test Specimens

The water–cement ratio of this specimen was 0.3. We carried out the following preparation steps: First, the corresponding raw materials and water of the cementitious early-strength anchoring material were weighed using a high-precision electronic balance (accurate to 0.01 g), and the material was poured into the mixing drum of a mixer and stirred for 1 min. Then, water was added during stirring, and stirring continued for 5 min. After the slurry was evenly mixed, the mixture was poured into a mold coated with a release agent, air bubbles were removed via the usual vibration method, and the mixture was allowed to stand at room temperature for 24 h before removing the mold. The specimen was then placed in a standard curing oven with constant temperature and humidity and cured for 28 days in an environment with a set temperature of (20 ± 3) °C and a relative humidity of (95 ± 2)%.

By referring to previous research [15–18] and following the size standards suggested by ASTM C39 [19], cylindrical specimens with a diameter of 50 ± 1 mm and a length-to-diameter ratio of 2.0 were made for mechanical performance testing, with no less than three parallel specimens prepared for each group of experiments. After the specimens were made, they were numbered and recorded according to the purpose of the test. The specimens were then cured until the required age (28 days) and taken out for further testing.

2.3. Setting of Bond Strength Test Specimens

(1) Specimen preparation

The specimen for the tensile test is shown in Figure 1a. The rock material used was granite from Qingdao, with dimensions of 15 cm × 15 cm × 18 cm. A hole with a diameter (d) of 3 cm and a depth of 130 mm was drilled in the center of the specimen surface, and a Φ15.2 mm steel strand with a length of 300 mm was chosen as the reinforcing body. This was a destructive test, and the anchoring agent's bond strength with the rock mass could only be measured after the anchoring body was pulled out. To avoid the steel strand being pulled out of the anchoring body, a compression sleeve with a diameter of 30 mm and a length of 30 mm was pressed onto the end of the steel strand using a crimping machine (the bonding length between the anchoring body and the rock mass was 100 mm). A compression sleeve was also set at the front end of the steel strand for clamping via the testing machine.

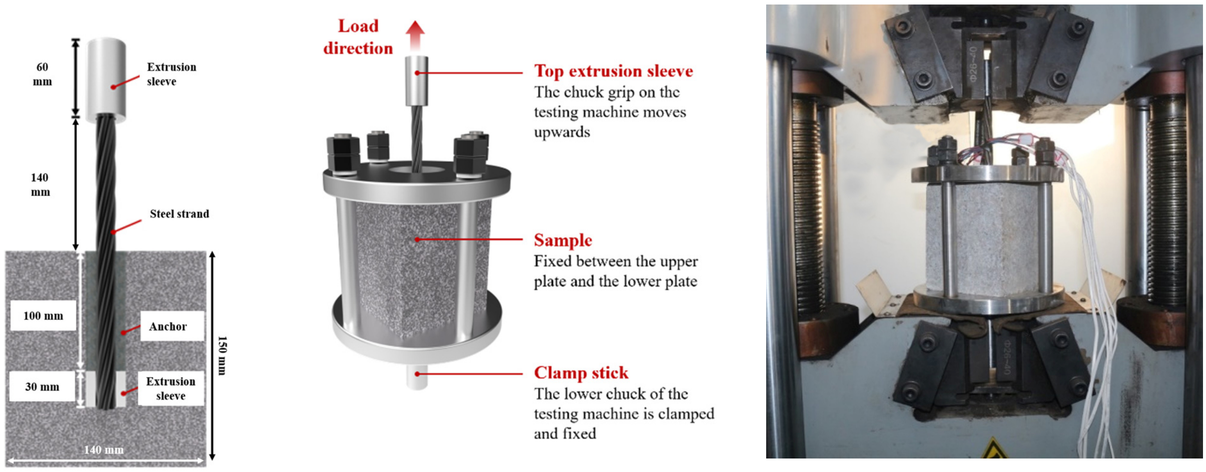

(**a**) Specimen preparation (**b**) Fixtures (**c**) Tensile test

Figure 1. Schematic diagram of tension sample and test device setup.

(2) Design of specimen fixation device

The fixation device is shown in Figure 1b and is made of No. 45 high-strength steel. During operation, the upper steel plate is removed vertically, and the prepared tensile specimen is placed into the device diagonally. The lower steel plate supports the specimen and connects the four threaded posts for load bearing. After the specimen is placed, the upper steel plate is threaded through the steel strand in the specimen in the original direction, so that the lower surface of the specimen is in contact with the upper surface of the rock. Then, washers and spring washers are placed and tightened diagonally with high-strength nuts.

(3) Tensile test

The loading device for this test was a WAW-1000B microcomputer-controlled electro-hydraulic servo universal testing machine from Forceleader, as shown in Figure 1c, with a range of 300 kN. This testing machine adopts a lower oil cylinder mainframe and is mainly used for tensile, compression, bending, and shear tests of various metal and non-metal materials, as well as some special tests of products.

2.4. Freeze–Thaw Cycling Test

The freeze–thaw cycling test in this study was carried out according to the methods for testing frost resistance of materials specified in ASTM C666 [20] and the "Standard Test Methods for Long-Term Performance and Durability of Ordinary Concrete" (GB/T50082-2009) [21]. Currently, there are two main methods for conducting freeze–thaw cycling tests on cementitious materials: rapid freezing and slow freezing [22,23]. The rapid freezing method uses a "water freezing and thawing" process, where the test samples are submerged in water during the entire testing process to simulate freeze–thaw cycles through ice formation and melting [5]. The slow freezing method uses an "air freezing and thawing" process, where the samples are exposed to both air and water during the testing process and freeze in the air before melting in water to simulate freeze–thaw cycles [24–26]. Considering the actual conditions faced by cement-based early-strength anchor material in grouting engineering, where the solidified body is exposed to a multiphase environment during service instead of a single liquid phase, and in order to better simulate the freeze–thaw environment in the winter season, this test adopted the "air freezing and thawing" process for cycling [27].

The test was conducted using the GDW-225 high- and low-temperature alternating humidity test chamber produced by Tianjin Gangyuan Testing Instrument Factory, with the main technical parameters shown in Table 3.

Table 3. Technical parameters of freeze–thaw cycle test equipment.

Machine Model	Temperature Range	Humidity Range	Temperature Deviation	Cooling Rate	Inner Box Size (mm)
GDW-225	−40~110 °C	20~98% RH	±2 °C	≥0.7~1.0 °C/min	500 × 600 × 750

As freeze–thaw cycling tests need to be conducted with samples saturated with water, cured samples need to be soaked in (20 ± 2) °C water to saturation before a freeze–thaw test. Before soaking, the dry weight of each sample needed to be measured. During soaking, we ensured that the water level was 2–3 cm above the top of the sample. We continuously tested the quality changes in the samples during soaking. According to the actual test results, the quality of the samples would no longer increase after being soaked in water for four days, which indicated that the samples had been saturated. After soaking, the saturated samples were removed, residual water on the surface was wiped off with a wet cloth, and the dry weight of the saturated surface of the sample was recorded, as well as the appearance of the sample.

The compressive strength specimens and bond strength specimens were placed in the center of the test box for freezing. The freezing time was recorded from the time when the temperature inside the box dropped to −18 °C, and the freezing time was 4 h. The air temperature in the freeze–thaw test box was maintained at −20 °C during the freezing period. After the freezing was completed, we immediately put the samples in water at 20 °C to melt, and the water level should have been 2–3 cm above the top of the sample. The melting time was 4 h. When the melting was completed, the freeze–thaw cycle was completed, and the next cycle began. The duration of each freeze–thaw cycle in this test was 8 h. The test was designed to conduct 5, 15, 25, 50, 75, and 100 freeze–thaw cycles. After the samples in each group reached the designated number of freeze–thaw cycles, they were taken out, and their appearance changes and residual weight were observed and recorded before strength tests were conducted on them.

3. Results

3.1. Microscopic Morphological Changes

Upon visual inspection of the cement-based early-strength anchor material samples after different freeze–thaw cycles, it was found that all groups of samples had trace amounts of pores on their surfaces. After 50 cycles, there was no significant increase in pore size, crack propagation, or peeling on the surface of the samples. After 75 cycles, slight shedding occurred at the edge of the samples. After 100 cycles, obvious chunky peeling appeared on the surface of the samples, and the external microcracks extended to a certain degree, but there were no large cracks or net-like cracks that could penetrate the sample.

To more intuitively observe the microscopic morphological changes in the cement-based early-strength anchor material after freeze–thaw cycling, fresh sections of the samples with different cycle numbers were selected after uniaxial compression testing and were observed and analyzed using a scanning electron microscope (SEM) at a magnification of 5000 times after freeze-drying. The scanning images are shown in Figure 2.

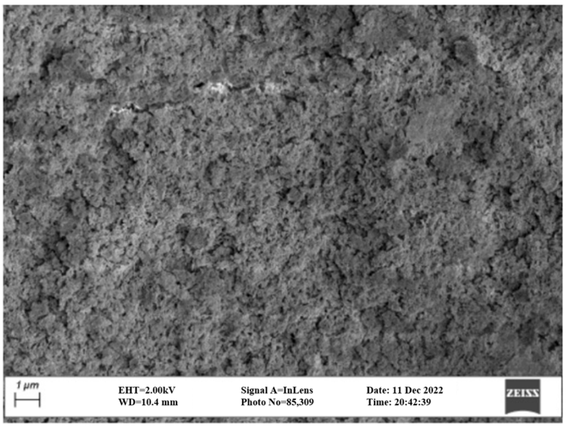

Freeze–thaw cycle 0 times (5000×)

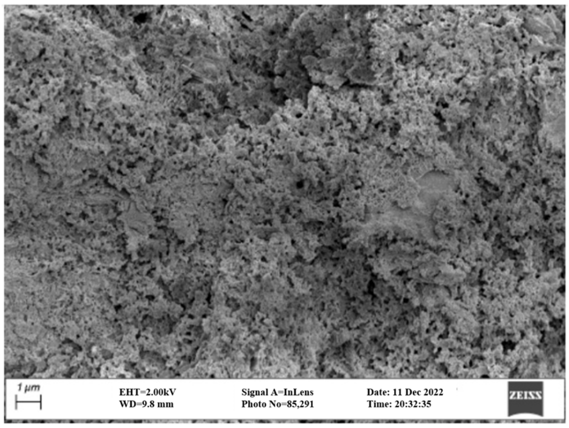

Freeze–thaw cycle 15 times (5000×)

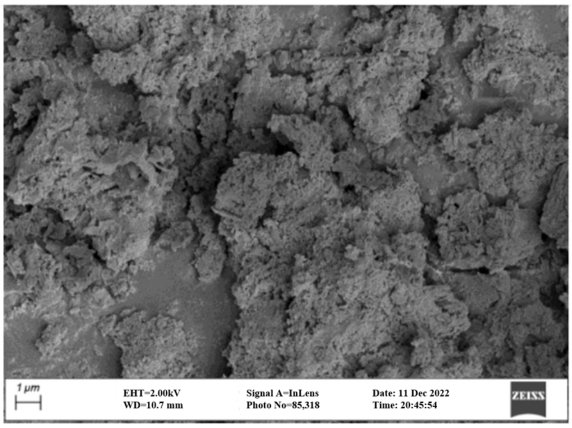

Freeze–thaw cycle 50 times (5000×)

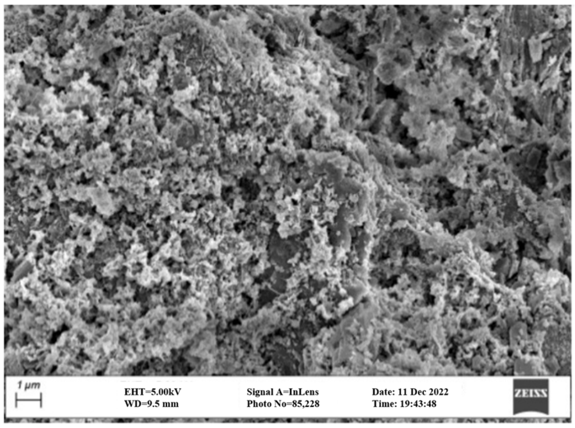

Freeze–thaw cycle 100 times (5000×)

Figure 2. SEM of cement-based early-strength anchor material agent specimens after freeze–thaw cycles.

The observation from Figure 2 shows that the surface of the non-frozen–thawed sample was relatively flat, with few pores and microcracks, high bond strength of the cement matrix, and tight contact between particles, indicating good microstructural density. After 15 freeze–thaw cycles, the surface showed slight protrusions and wrinkles, and there was a slight increase in pore size and quantity, but no obvious crack development was observed. After 50 cycles, the surface became rougher, and the bond strength of the cement matrix decreased, resulting in a reduction in the effective contact area between particles. At the same time, blocky cracking and layering of microcracks were observed, leading to reduced density. When the freeze–thaw cycle reached 100 times, due to the repeated freezing and thawing of water, combined with the joint action of frost heaving, compression and water seepage, the surface of the sample became uneven, with a significant increase in pore structure and microcrack interconnectivity. The originally dense cement matrix structure became "leaky", and "tearing" and peeling occurred locally. The microstructural mechanism of freeze–thaw damage to the cement-based early-strength anchor material sample can be summarized in Figure 3. Figure 3 shows that under the continuous accumulation of the number of freeze–thaw cycles, the original bonding relationship of the material was further destroyed due to the action of water, and some cracks and fine holes appeared. Cracks and holes further expanded with the freeze–thaw cycle, and after connection, the material fell off locally, causing the material to deteriorate continuously.

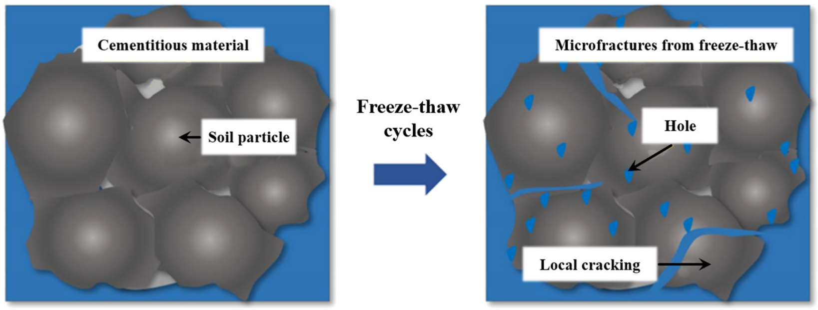

Figure 3. Micro-mechanism of influence of freeze–thaw cycles on cement-based early-strength anchor material agent specimens.

The freezing and thawing cycles weakened the overall microstructure of the cement-based early-strength anchor material, causing a loss in quality and a decrease in the mechanical strength of the sample on a macroscopic level. In future studies on improving the frost resistance of cement-based early-strength anchor material, appropriate materials can be added to the raw material to enhance the bonding of the cementitious material in the freezing and thawing environment, increase the bonding area between materials, reduce the migration of water, and maintain the integrity of the interface.

3.2. Compressive Strength

Compressive strength is closely related to other mechanical and deformation parameters, such as tensile strength, elastic modulus, and peak strain, and it is the most important indicator for testing the mechanical properties of cementitious materials [28]. In order to evaluate the mechanical properties of the cement-based early-strength anchor material after freeze–thaw cycles, uniaxial compression tests were carried out on the cement-based early-strength anchor material samples treated with different freeze–thaw cycles, and the average compressive strength variation with freeze–thaw cycles was obtained, as shown in Figure 4. After 5, 15, 25, 50, 75, and 100 freeze–thaw cycles, the average compressive strengths of the samples were 26.63 MPa, 26.02 MPa, 24.95 MPa, 23.13 MPa, 21.51 MPa, and 20.49 MPa, respectively. Compared with the 0-cycle group that did not undergo freeze–thaw cycles with a compressive strength of 28.31 MPa, the compressive strength of the samples decreased by 5.94%, 8.11%, 11.88%, 18.30%, 24.03%, and 27.62%, respectively. It can be seen that freeze–thaw cycles led to a deterioration in the compressive strength of the cement-based early-strength anchor material samples, and the compressive strength showed a gradual decrease trend with the increase in the number of freeze–thaw cycles.

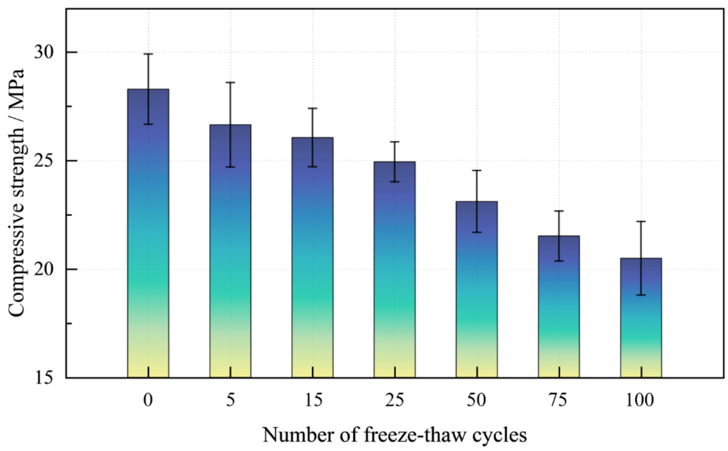

Figure 4. Changes in mean compressive strength of cement-based early-strength anchor material agent after different freeze–thaw cycles.

3.3. Stress–Strain Relationship

The stress–strain relationship reflects a material's fundamental mechanical properties and is the primary basis for studying its mechanical strength and deformation characteristics [29]. In order to have a more intuitive understanding of the effect of freeze–thaw cycles on the strength and deformation of the cement-based early-strength anchor material, the stress–strain curves of the saturated specimens in each group of the experiment were compared under uniaxial compression testing. The results are shown in Figure 5. The compressive stress–strain curve of the cement-based early-strength anchor material specimen can be divided into four stages: the dense compression stage, the elastic growth stage, the yield stage, and the residual stage. During the initial compression stage, the specimen's internal pores were gradually compacted and reduced, the specimen's stiffness increased, and the curve showed an upward concave shape. The curve grew approximately linearly as compression continued, indicating that the specimen entered the elastic stage. When compression reached a certain degree, the curve no longer changed linearly. At this point, the internal damage to the specimen intensified, and the curve became concave, entering the yield stage. When the stress reached the peak value, the specimen failed, and the curve changed sharply. We continued to load the specimen, and the stress no longer increased, while the strain continued to increase, entering the residual stage. During the compression process, the stress–strain curve of the cement-based early-strength anchor material specimen showed a strain-softening type. After the stress reached the peak value, the specimen underwent brittle fracture, and the stress value dropped rapidly. As the number of freeze–thaw cycles increased, the compressive stress–strain curve of the cement-based early-strength anchor material specimen gradually decreased in the growth stage before yield, and the yield stage curve gradually flattened, with significant decreases in peak stress and curve slope. We believe that this was caused by the deterioration of the bonding relationship of the material by the freeze–thaw cycle; with the increase in the number of freeze–thaw cycles, at the microscopic level, the bonding relationship between the material particles was further destroyed under the action of the intermolecular force of water, resulting in microcracks and holes, and with the increasing number of freeze–thaw cycles, the holes and cracks continued to expand, further deteriorating the bonding relationship between the material particles. This resulted in a mechanical reduction in the maximum stress value to which the material was subjected. At the same time, the material no longer underwent the crack generation-propagation stage when it was pressed, but the existing cracks directly began to propagate, which corresponded to the gradual decrease in the slope of the stress–strain curve in the stage before the yield of the material mentioned above.

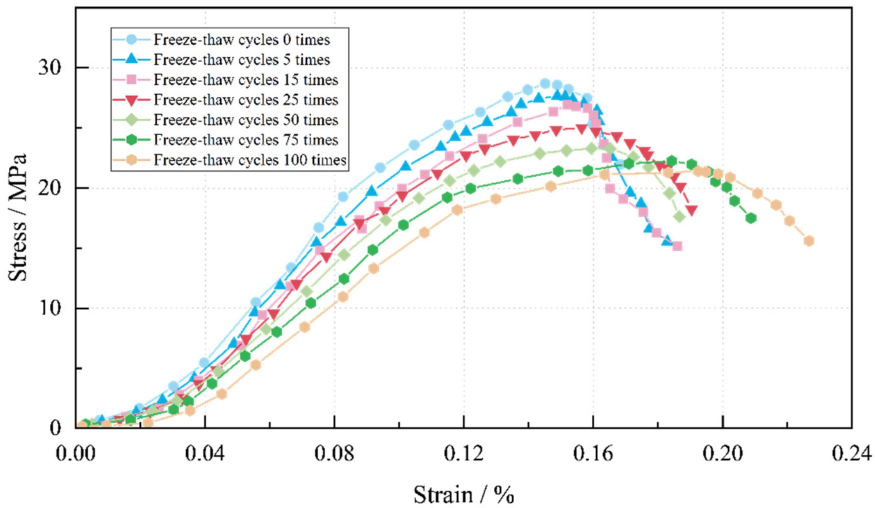

Figure 5. Compressive stress–strain curve of cement-based early-strength anchor material after freeze–thaw cycles.

The peak strain is an important indicator reflecting the deformation ability and can be used to analyze the deformation characteristics of cement-based adhesive materials. The peak strain of each group of samples in the characteristic stress–strain curve was selected, and the ratio of the peak strain after freeze–thaw cycling to that of the control group (0 cycles) is listed in Table 4. The variation in the peak strain ratio with the number of freeze–thaw cycles was obtained and is shown in Figure 6.

Table 4. Peak strain of specimens after freeze–thaw cycles.

Freeze–Thaw Cycle Number	Peak Strain	$\varepsilon_D/\varepsilon_0$
0	0.14531%	1
5	0.14875%	1.023674
15	0.15219%	1.047347
25	0.15625%	1.075287
50	0.16469%	1.13337
75	0.18375%	1.264538
100	0.19250%	1.324754

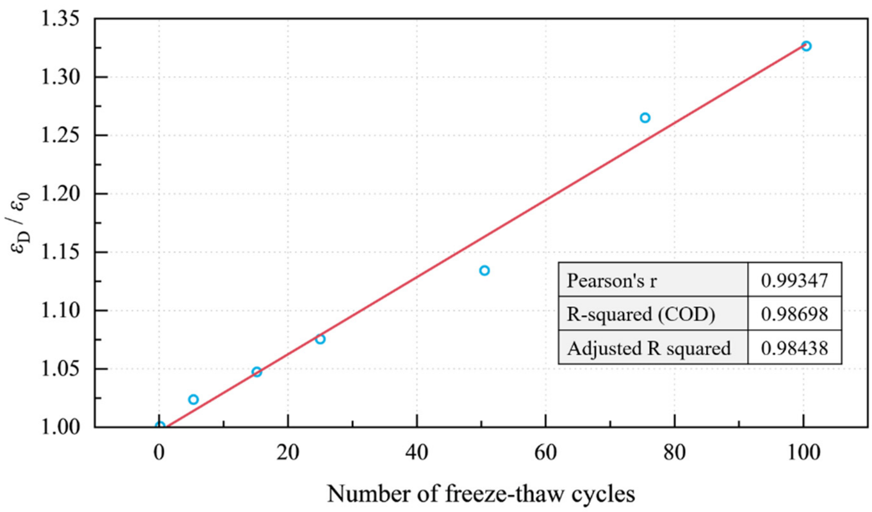

Figure 6. Changes in the peak strain ratio of specimens with freeze–thaw cycles.

According to the experimental data, the strain at which the sample reached the peak stress gradually increased with the number of freeze–thaw cycles, and the peak strain ratio was linearly correlated with the number of freeze–thaw cycles. Freeze–thaw cycling caused the internal pore water of the saturated sample to switch between ice and water phases, and the compressive force generated by volume expansion and contraction and the seepage force generated by water flow constantly damaged the internal structure of the sample. This led to an increase in the deformation when the sample reached its peak failure with an increase in the number of freeze–thaw cycles.

4. Discussion

4.1. The Effect of Freeze–Thaw Cycling on Bond Strength

The calculation of ultimate bond strength in this paper is based on the average shear stress theory. The ultimate average bond strength is calculated using the peak load during the tension process using the testing machine, as shown in Equation (1):

$$\tau_{mA} = \frac{F_m}{\pi d l} \cdot 10^{-3} \quad (1)$$

where:

τ_{mA}—ultimate average bond strength (MPa);
F_m—ultimate load (kN);
d—diameter of the anchor (m);
l—length of the anchor (m).

Based on the test results under normal curing conditions, the maximum bearing capacity of the cement-based early-strength anchor material bonded to the granite specimen interface was 60.32 kN. The maximum bearing capacities after 25, 50, 75, and 100 freeze–thaw cycles were 53.70 kN, 49.39 kN, 47.12 kN, and 45.36 kN, respectively. The load–displacement curves of each test block after freeze–thaw cycles are shown in Figure 7. It can be seen from the figure that with the increase in the number of freeze–thaw cycles, the compressive strength of the test block gradually decreased, and the two were positively correlated, and the maximum reduction in the test block strength was about 25%. Considering the microscopic performance of the test block after a freeze–thaw cycle, microcracks occurred in the test block due to the freeze–thaw cycle, and these microcracks continued to expand and expand with the increase in the number of freeze–thaw cycles, which further destroyed the interparticle bonding structure of the test block, so that the compressive strength of the test block decreased with the increase in the number of freeze–thaw cycles.

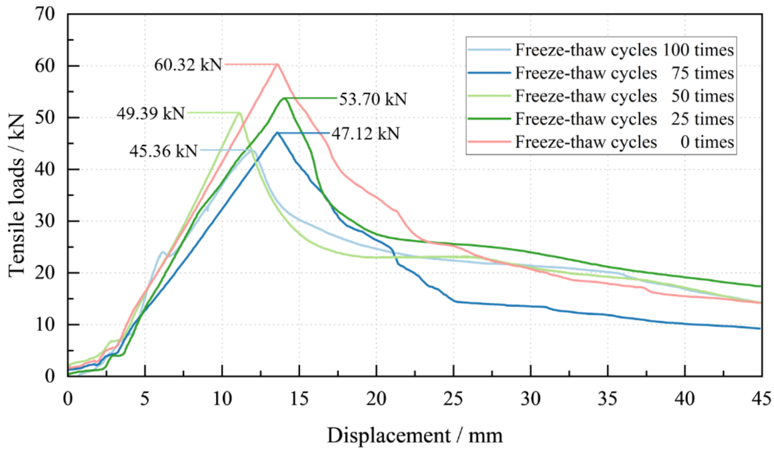

Figure 7. Load–displacement curve of each test block after freeze–thaw cycle.

The change in bond strength with the number of freeze–thaw cycles calculated according to Formula (1) is shown in Figure 8. According to the data in the figure, it can be seen that the bond strength between the cement-based early-strength anchor material and granite gradually decreased with the increase in the number of freeze–thaw cycles.

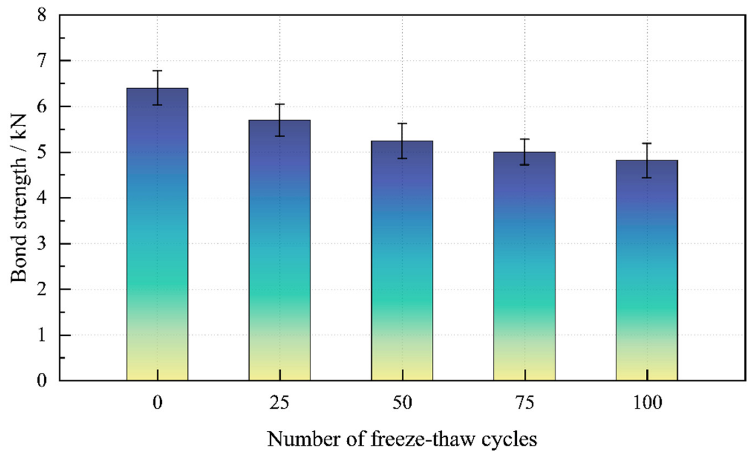

Figure 8. Changes in bond strength with the number of freeze–thaw cycles.

4.2. Assessment of Damage Degree after Freeze–Thaw Cycling

In order to more intuitively assess the degree of damage to the cement-based early-strength anchor material samples after freeze–thaw cycling in this experiment, referring to the relevant content on freeze–thaw damage in Specification [21], the standard for the damage to the cement-based early-strength anchor material samples after freeze–thaw cycling is defined as a mass loss rate of 5% or a bonding strength decrease to 75%. Since there are certain errors and limitations in evaluating durability based on a single factor, a damage index ω [30] that can represent the degree of sample damage after freeze–thaw cycling is defined in combination with the damage criteria. The expression is:

$$\omega = 1 \pm \frac{5\% - s_1}{5\%} \cdot \frac{\Delta f_c - 75\%}{25\%} \tag{2}$$

where S_1 is the mass loss rate of the sample after freeze–thaw cycling, and Δf_c is the percentage of the residual bonding strength of the sample after freeze–thaw cycling. When $S_1 > 5\%$ and $\Delta f_c < 75\%$, the result is marked as "+"; otherwise, it is marked as "−".

Based on the freeze–thaw test data, the relationship between the ω value and the number of freeze–thaw cycles is shown in Figure 9. The ω value comprehensively reflects the damage caused by mass loss and strength loss during freeze–thaw cycles and can be used to determine the degree of damage to the specimen through experimental measurement, which is influenced by the mass loss rate and bond strength loss rate [31]. According to Equation (3) and Figure 9, when the ω value is 0, it means that the specimen has not been damaged by freeze–thaw cycles; the smaller the ω value, the lesser the degree of damage caused by freeze–thaw cycles, and the larger the value, the greater the degree of damage. According to the specimen failure criteria defined in this experiment, when $\omega \geq 1$, the specimen is considered to have failed due to freeze–thaw effects. In this experiment, the degree of damage, or the ω value, of the cement-based early-strength anchor material specimen increased with the number of freeze–thaw cycles experienced, and the relationship between the degree of damage ω value and the number of freeze–thaw cycles was obtained by fitting, which can be expressed as:

$$\omega = A \cdot N^{\frac{1}{2}} + B \tag{3}$$

where A and B are parameters related to freeze–thaw tests, $A = 0.112 \pm 0.005$ and $B = -0.038 \pm 0.03$; N represents the number of freeze–thaw cycles, and the curve fitting is good. According to Formula 3it can be seen that the cement-based early-strength anchor material specimen in this experiment had $\omega \geq 1$ after approximately 86 freeze–thaw cycles. That is, the frost resistance of the cement-based early-strength anchor material specimen within 85 freeze–thaw cycles in this experiment can be considered as good.

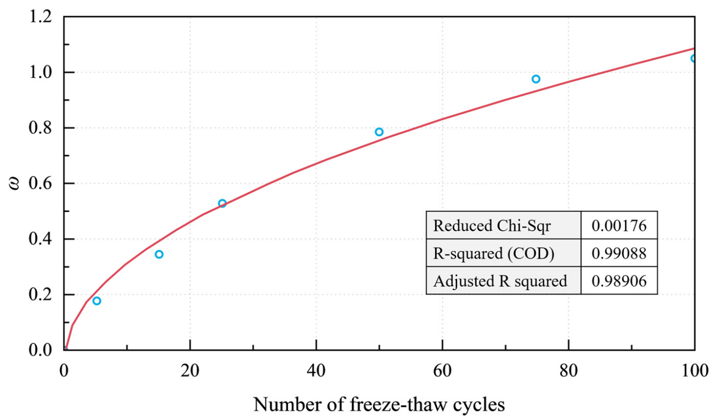

Figure 9. Damage degree of the cement-based early-strength anchor specimens after freeze–thaw cycles.

5. Conclusions

This study mainly analyzes the results of the freeze–thaw cycle test under the harsh environment of a simulated permafrost region. By analyzing the changes in the appearance, mass loss, failure mode, macro-mechanical properties, and microstructure of the cement-based early-strength anchor material samples treated with different freeze–thaw cycle numbers, the evolution laws and micro-mechanisms of the material's mechanical properties after freeze–thaw cycles are explained. The following main conclusions are drawn:

(1) After 5, 15, 25, 50, 75, and 100 freeze–thaw cycles, the average compressive strength of the samples decreased by 5.94%, 8.11%, 11.88%, 18.30%, 24.03%, and 27.62%, respectively, compared with the control group without freeze–thaw cycles. The compressive strength showed a decreasing trend with the increase in the cycle number.
(2) As the freeze–thaw cycles increased, the growth segment of the curve before reaching the yield point decreased gradually, and the curve in the yield segment became smoother. The strain at the peak stress of the sample increased with the increase in the freeze–thaw cycle number, and the ratio of peak strain to initial strain $\varepsilon D/\varepsilon 0$ was linearly related to the cycle number. After reaching the peak stress, the sample underwent brittle failure.
(3) The SEM analysis shows the surface of the sample without freeze–thaw treatment was relatively flat, with fewer pores and microcracks, a higher bonding degree of the cementing material, tighter contact between particles, and good microstructure compactness.
(4) Freeze–thaw cycles cause continuous switching of the internal pore water between ice and water, and the extrusion force generated by volume expansion and contraction and the seepage force generated by water flow continuously damage the internal structure of the sample, making the deformation at the peak damage of the sample increase with the increase in the freeze–thaw cycle number, and the stiffness of the sample and its ability to resist deformation decrease.
(5) In subsequent studies on frost resistance improvement, appropriate materials can be added to strengthen the connection between cementing materials in the freeze–thaw environment, increase the contact bonding area between materials, and weaken the migration of water to maintain the integrity of the interface.
(6) In this paper, the effect of freeze–thaw cycles on cement-based early-strength anchorage materials was studied. There is still something to be desired. For example, the number of freeze–thaw cycles was still relatively small in comparison to reality. Due to equipment limitations, the temperature range in the freeze–thaw cycle was small, which means it was difficult to reflect the performance of a specimen in extreme cases, etc.

Author Contributions: Data curation, Z.D. and M.Y.; funding acquisition, S.D.; investigation, Z.D.; methodology, M.Y.; project administration, M.Y., S.D. and Z.D.; writing—original draft, M.Y.; writing—review and editing, Z.D., S.D. and M.Y. All authors contributed to the article and approved the submitted version. All authors have read and agreed to the published version of the manuscript.

Funding: This research received no external funding.

Institutional Review Board Statement: Not applicable.

Informed Consent Statement: Not applicable.

Data Availability Statement: The data used to support the findings of this study are included within the article.

Acknowledgments: We appreciate the reviewers for their valuable comments, which are crucial to shaping our manuscript. At the same time, we are also grateful for the financial support provided by the above-mentioned funds.

Conflicts of Interest: The authors declare that the research was conducted in the absence of any commercial or financial relationships that could be construed as a potential conflict of interest.

References

1. Shi, S. The influence of freeze-thaw cycles on the mechanical properties of concrete. *J. Civ. Eng.* **1997**, *30*, 8.
2. Yan, L.; Xiong, W.; Wang, X. Application and practice of double-liquid grouting in anchor cable construction under complex geological conditions in alpine areas. In Proceedings of the 16th National Water Conservancy and Hydropower Foundation and Foundation Engineering Academic Exchange Conference, Wuhan, China, 16 December 2021.
3. Li, J. Experimental Study on Freezing and Thawing Damage Mechanism of Rocks in Cold Regions Based on NMR Technology. Ph.D. Thesis, Central South University, Changsha, China, 2012.
4. Li, V.; Lepech, M. Crack resistant concrete material for transportation construction. In Proceedings of the TRB83rd Meeting, Washington, DC, USA, 11–15 January 2004.
5. Najjar, S.; Moghaddam, A.M.; Sahaf, A.; Aliha, M.R.M. Experimental and statistical exploring for mixed-mode (I&II) fracture behavior of cement emulsified asphalt mortar under freeze–thaw cycles and aging condition. *Theor. Appl. Fract. Mech.* **2022**, *122*, 103643.
6. Chen, J.; Zhao, C.; Liu, Q.; Shi, X.; Sun, Z. Investigation on frost heaving stress (FHS) of porous cement concrete exposed to freeze-thaw cycles. *Cold Reg. Sci. Technol.* **2023**, *205*, 103694. [CrossRef]
7. Zhang, N.; Liao, J.; Zhang, T.; Ji, W.Z. The thermal deformation of cement-based Material at low temperatures. *Adv. Mater. Res.* **2015**, *1081*, 279–283. [CrossRef]
8. Alsaif, A.; Bernal, S.; Guadagnini, M.; Pilakoutas, K. Freeze-thaw resistance of steel fibre reinforced rubberised concrete. *Constr. Build. Mater.* **2019**, *195*, 450–458. [CrossRef]
9. Johannesson, B. Dimensional and ice content changes of hardened concrete at different freezing and thawing temperatures. *Cem. Concr. Compos.* **2010**, *32*, 73–83. [CrossRef]
10. Powers, T.C. A Working Hypothesis for Further Studies of Frost Resistance of Concrete. *J. Proc.* **1945**, *41*, 245–272.
11. Powers, T.C.; Helmuth, R.A. Theory of Volume Changes in Hardened Portland Cement Paste during Freezing. *Proc. Highw. Res. Board* **1953**, *32*, 285–297.
12. Wang, Y.; Xu, L. Research progress on the influence of cement particle size distribution on cement performance. *Mater. Rev.* **2010**, *24*, 68–71.
13. Zhang, Y.; Wang, H.; Liu, T.; Liu, H.; Deng, S. Interpretation of pore pressure dissipation of CPTu in intermediate soil considering partial drainage effect. *Ocean Eng.* **2022**, *266*, 112956. [CrossRef]
14. Zhang, Y.; Feng, X.; Deng, S.; Ding, C.; Liu, T. Pore Pressure Response and Dissipation of Piezocone Test in Shallow Silty Soil of Yellow River Delta. *J. Mar. Sci. Eng.* **2022**, *10*, 225. [CrossRef]
15. Yi, S.T.; Kim, J.K.; Oh, T.K. Effect of strength and age on the stress–strain curves of concrete specimens. *Cem. Concr. Res.* **2003**, *33*, 1235–1244. [CrossRef]
16. Amiri, M.; Moomivand, H. Development of a new physical modeling method to investigate the effect of porosity on the parameters of intact rock failure criteria. *Arab. J. Geosci.* **2019**, *10*, 12. [CrossRef]
17. Li, S.; Liew, J.R. Experimental and Data-Driven analysis on compressive strength of steel fibre reinforced high strength concrete and mortar at elevated temperature. *Constr. Build. Mater.* **2022**, *341*, 127845. [CrossRef]
18. Cui, L. Experimental and Numerical Investigation on Static and Dynamic Characteristics of Cylindrical Concrete Specimens. Ph.D. Thesis, Hunan University, Changsha, China, 2016.
19. *ASTM C39*; Standard Test Method for Compressive Strength of Cylindrical Concrete Specimens. ASTM International: West Conshohocken, PA, USA, 2012.
20. *ASTM C666*; Standard Test Method for Resistance of Concrete to Rapid Freezing and Thawing. ASTM International: West Conshohocken, PA, USA, 2015.
21. *GB/T 50082-2009*; General Technical Specification for Long-Term Performance and Durability Test Methods of Ordinary Concrete. China Architecture & Building Press: Beijing, China, 2009.
22. Zhang, Y.; Feng, X.; Ding, C.; Liu, Y.; Liu, T. Study of Cone Penetration Rate Effects in the Yellow River Delta Silty Soils with Different Clay Contents and State Parameters. *Ocean Eng.* **2022**, *250*, 110982. [CrossRef]
23. Zhang, Y.; Lu, Y.; Liu, T. Undrained Horizontal-Moment Bearing Capacity of Caisson Foundations in Over-consolidated Clay Considering Effects of Gap. *Mar. Georesour. Geotechnol.* **2019**, *39*, 255–266. [CrossRef]
24. Jia, L.; Nuliyamu, X.; Chen, C.; Guo, J.; Bao, D. Study on frost resistance of fast-hardening magnesium phosphate-iron-aluminum compound cement. *J. Glaciol. Geocryol.* **2022**, *44*, 1021–1028.
25. Kou, J.; Hu, J.; Ma, M.; Yu, D. Experimental study on mechanical properties of cement-based grouting material under combined action of chloride ions and freeze-thaw erosion. *Build. Struct.* **2020**, *50*, 100–105.
26. Liu, Y. Research on Frost Resistance of Concrete in High-Altitude Cold Areas. Ph.D. Thesis, Xi'an Technological University, Xi'an, China, 2021.
27. Wu, F.; Cui, L.; Yang, J.; Bian, Q. Study on the anti-salt-freeze-thaw performance of potassium magnesium phosphate cement slurry. *Bull. Chin. Ceram. Soc.* **2018**, *37*, 686–694.
28. Jia, B. Study on the Static and Dynamic Properties of Concrete under High Temperature. Ph.D. Thesis, Chongqing University, Chongqing, China, 2011.

29. Duan, A. Study on the Constitutive Relationship of Frozen-Thawed Concrete and Numerical Simulation of Freeze-Thaw Process. Ph.D. Thesis, Tsinghua University, Beijing, China, 2009.
30. *ASTM C469/C469M*; Standard Test Method for Static Modulus of Elasticity and Poisson's Ratio of Concrete. ASTM International: West Conshohocken, PA, USA, 2022.
31. Mu, R. Durability and Life Prediction of Concrete under Freeze-Thaw Cycles and Combined Effects of External Flexural Stress and Salt Solution. Ph.D. Thesis, Southeast University, Xiamen, China, 2000.